Progress In Electromagnetics Research Letters, Vol. 107, 159–167, 2022

Gain and Bandwidth Enhancement of a CPW-Fed Bidirectional Dumbbell Shaped Slot Antenna Using PRS

Ameet M. Mehta[1, 2, *], Shankar B. Deosarkar[1], and Anil B. Nandgaonkar[1]

Abstract—A bidirectional, coplanar waveguide (CPW) fed dumbbell-shaped slot antenna with partially reflecting surface (PRS) with parasitic patches for gain, bandwidth, and radiation pattern improvement is investigated. A dumbbell-shaped CPW-fed slot antenna has a dimension of $0.71\lambda_g \times 0.71\lambda_g \times 0.0571\lambda_g$. The proposed antenna is simple in design and has low profile structure. To achieve improvement in bandwidth, gain, and bidirectional radiation pattern, PRS with parasitic patches are placed on top and bottom of antenna at a distance of $0.25\lambda_g$. The proposed design yields wide bandwidth of 4.11 GHz (4.48–8.59 GHz) with percentage bandwidth of 62.89%, $S_{11} \leq -10$ dB, and peak gain of 5.61 dBi. The variation in the gain over desired bandwidth is less than 3 dB. The antenna is fabricated using an FR4 substrate with relative permittivity of 4.4. The measured results corroborate the design and stipulate the proposed structure to be suitable for applications in C band.

1. INTRODUCTION

The C band has a variety of applications such as WLAN and RFID [1–4]. The frequency of the C band ranges from 4 to 8 GHz and houses important standards like IEEE802.11a and HIPERLAN/2. These standards accommodate data rate up to 54 Mbps in 5 GHz ISM band [1, 2]. The IEEE 802.11a defines bands from 5.15 to 5.25 GHz, 5.25 to 5.35 GHz, and 5.725 to 5.825 GHz [4]. HIPERLAN/2 defines a band from 5.15 to 5.35 GHz and 5.47 to 5.725 GHz [1, 3]. Another important application in this band is Radio Frequency Identification (RFID) which uses 5.8 GHz band. The Sub-6 GHz band is also used for 5G mobile communication.

Low-profile antennas like microstrip antenna (MSA) and coplanar waveguide (CPW) fed slot antennas are used in applications where size, cost, weight, performance, and simplicity in design are constraints. MSA provides narrow bandwidth, and the structure is generally in terms of $\lambda/2$ times the resonating frequency [5]. The problem of narrow bandwidth can be overcome by creating slots in the patch or other techniques as presented in [6–10]. Generally, it is found that the perimeter of the slot ring is $1.5\lambda_g$, and the perimeter of the feed line is λ_g [11, 12]. The length of the dipole patch is $0.5\lambda_g$ for capacitive type feed [13].

Over the years, partially reflecting surfaces (PRSs) with one or more layers of periodic patches on a dielectric substrate known as a frequency selective surface (FSS) is used efficiently as a superstrate which leads to low-profile resonant cavity antenna (RCA) devices [14–16]. The study of PRS as metamaterial was first proposed in [14]. The wideband capabilities of FSS layer like PRS were investigated in [15] but the available bandwidth is limited by the intrinsic characteristics of the magnitude and phase of the reflection characteristics of the single layer FSS based PRS designs. Several techniques for linearly polarised antennas for gain and bandwidth enhancement using PRS have been investigated [17–19]. High directivity antenna using PRS as a superstrate at a distance of $\lambda_0/4$ from ground plane is investigated

Received 15 September 2022, Accepted 8 November 2022, Scheduled 22 November 2022

* Corresponding author: Ameet M. Mehta (amehta.dbatu@gmail.com).

[1] Department of Electronics and Telecommunication Engineering, Dr. Babasaheb Ambedkar Technological University, Lonere, India.

[2] Department of Electronics and Telecommunication Engineering, Pillai College of Engineering, New Panvel, Raigad, India.

in [20]. FSS single layer on single side has been studied in [24–31], and the FSS layer increases the gain considerably but also makes the antenna design bulky and complex. A 7×7 FSS element array is used which increases the complexity of the antenna structure [26]. FSS elements on both sides of substrate have been studied in [27, 28]. A 4×4 FSS element array is placed at the bottom of the antenna [27]. A 5×5 FSS element array is placed on top of the antenna structure [28]. This placement improves the gain, but percentage bandwidth is greatly affected. A CPW-fed wideband RCA with two layer PRS superstrate has been studied in [30].

Certain areas like corridors, elevators, railways, and tunnels, where the movement of mobile users is along the straight path bidirectional antenna is preferred in order to achieve maximum efficiency [22]. To achieve bidirectional characteristics, two unidirectional antennas are installed in opposite planes, or two radiating elements are placed back to back. Placing two unidirectional antennas in opposite direction not only increases the volume but also has certain design complexities. There also arises a problem with feeding network, and such designs are also prone to have mutual coupling effects.

In this paper, a bidirectional, CPW-fed dumbbell-shaped slot antenna with PRS with parasitic patches for gain, bandwidth, and radiation pattern improvement is proposed. At first, the PRS with parasitic patches are placed on top of the antenna, and then the PRS with parasitic patches is placed on top as well as at the bottom of the antenna. The basic dumbbell antenna design resonates between 4.32- and 8.47 GHz with bandwidth of 4.15 GHz and maximum gain of 3.18 dBi. A bandwidth of 4.1 GHz (4.5–8.6 GHz) and a maximum gain of 5.5 dBi are achieved by placing PRS with parasitic patches on top of the antenna. When PRS with parasitic patches are placed on top as well as at bottom of the antenna, the bandwidth obtained is 4.12 GHz (4.55–8.67 GHz) with maximum gain of 6.05 dBi. The fabrication and testing of prototype antenna are done, and a good agreement is obtained between the simulated and measured results.

2. DESIGN OF ANTENNA

The geometry of the proposed CPW-fed slot antenna is as shown in Fig. 1. The fabrication of the antenna is done using an FR4 substrate with relative permittivity of 4.4 and loss tangent value around 0.02. FR4 substrate provides ease in manufacturing and is less expensive. The antenna substrate has dimensions of $0.71\lambda_g \times 0.71\lambda_g \times 0.0571\lambda_g$, where λ_g is the guided wavelength calculated at the first resonating frequency using following equations.

$$At\ First\ Resonating\ Frequency\ \lambda_0 = \frac{c}{f} \tag{1}$$

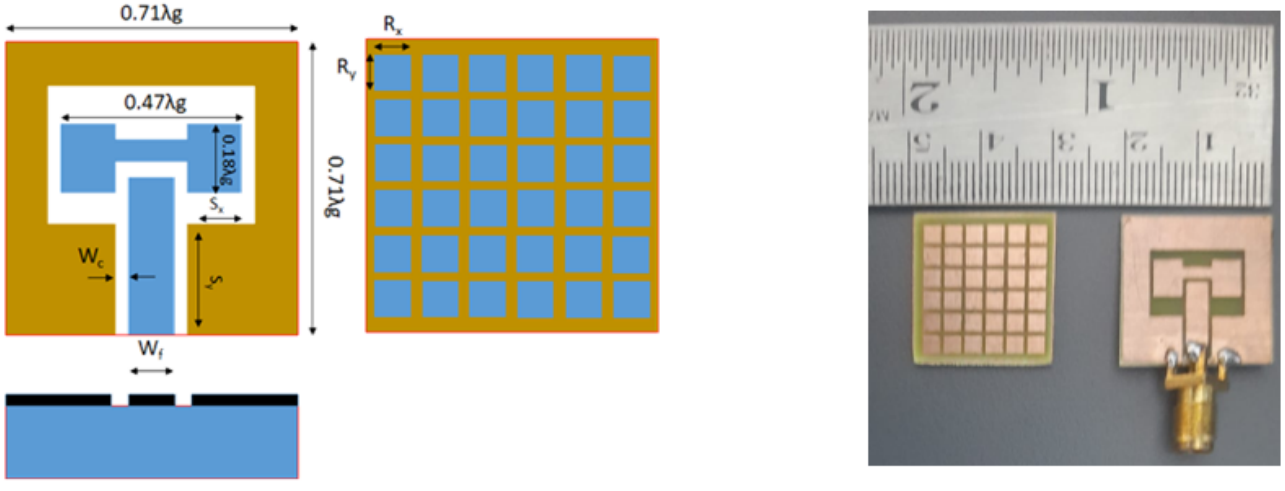

(a) (b) (c)

Figure 1. Geometry of the proposed antenna. (a) CPW fed dumbbell shaped slot antenna. (b) PRS with parasitic patches. (c) Fabricated prototype.

Calculate the value of guided wavelength

$$At\ First\ Resonating\ Frequency\ \lambda_g = \frac{\lambda_0}{\sqrt{\varepsilon_{eff}}} \tag{2}$$

A dumbbell-shaped dipole patch is etched in the slot layer. The slot is fed by CPW feeding structure. The perimeter of the rectangular slot is $1.64\lambda_g$. The CPW feedline is capacitive feed designed for 50-Ω characteristic impedance. The strip line has a width of W_f, and the spacing between the strip line and coplanar ground plane is W_c. The proposed antenna is designed in CST Studio Suite 2021 and has a uniform thickness of 0.035 mm.

The dumbbell-shaped MSA has dimensions of $0.47\lambda_g \times 0.18\lambda_g$. The length Sy is varied to get parametric analysis, and S_{11} is plotted for varying Sy, shown in Fig. 2(a). The value of Sy is varied from 6.1 mm to 6.6 mm, and the value selected is 6.2 mm.

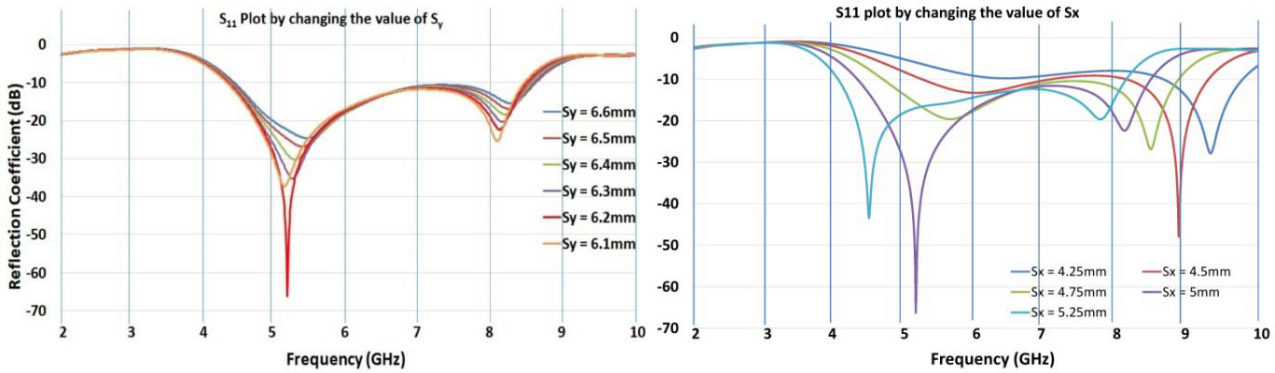

(a) (b)

Figure 2. S_{11} plot for parametric analysis. (a) S_{11} plot by varying Sy. (b) S_{11} plot by varying Sx.

The length of Sx is varied to get the parametric analysis; S_{11} is plotted for varying Sx and shown in Fig. 2(b). The value of Sx is varied from 4.25 mm to 5.25 mm; the value selected is 5 mm. The S_{11} plot shows that the lowest resonating frequency is 5.15 GHz, while the bandwidth obtained is 4.15 GHz between $f_1 = 4.32$ GHz and $f_2 = 8.47$ GHz. The maximum gain obtained from the design is 3.18 dBi at 7.6 GHz.

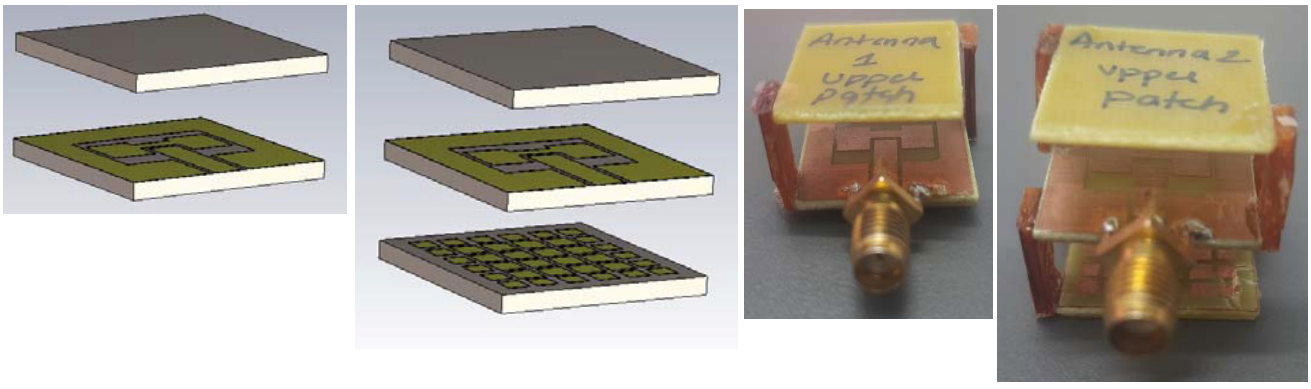

(a) (b) (c) (d)

Figure 3. Geometry of the proposed antenna with PRS with parasitic patch. (a) Antenna with PRS with parasitic patches on top. (b) Antenna with PRS with parasitic patches on top and bottom. (c) Fabricated prototype of antenna with PRS with parasitic patches on top. (d) Fabricated prototype of antenna with PRS with parasitic patches on top and bottom.

2.1. Antenna with PRS with Parasitic Patches

The PRS with parasitic patch is designed on the FR4 substrate with relative permittivity of 4.4 and loss tangent value around 0.02. The patch has a dimension of 2.5 mm, and the gap between two patches is 0.5 mm. The patch is placed on single as well as both sides of the antenna. The simulation is performed, and parametric analysis is done with regards to the distance between the antenna and PRS with parasitic patches, and the distance considered is $\lambda_g/4$ between the antenna and the patches. Fig. 3(a) shows the proposed antenna with PRS with parasitic patches on top. Fig. 3(b) shows the proposed antenna with PRSs with parasitic patches on top and bottom, while Fig. 3(c) and Fig. 3(d) show the fabricated prototypes.

Parametric analysis with regards to the distance between the patches and the patch size is simulated. Fig. 4(a) shows S_{11} plot by varying the distance between the patches and the antenna, and the value selected is $dx = 7$ mm. Fig. 4(b) shows S_{11} plot by varying the width of patches Rx. The best results are obtained at $Rx = Ry = 2.5$ mm.

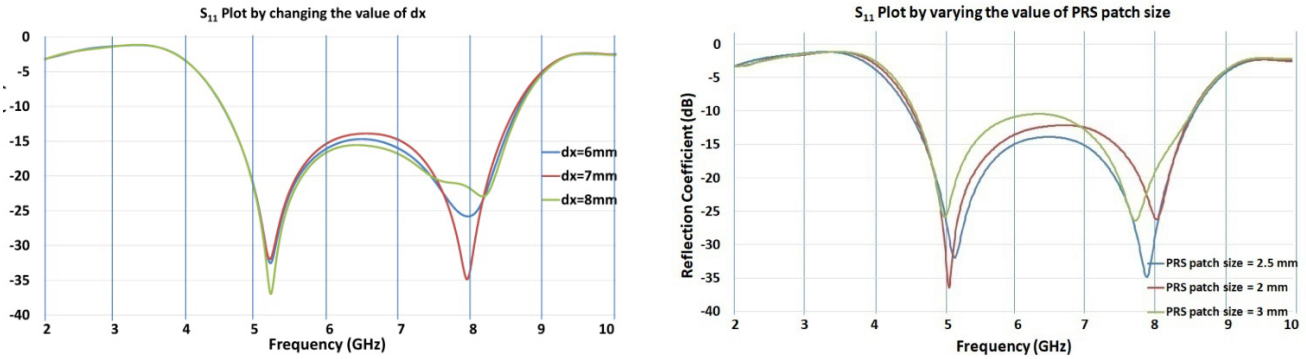

Figure 4. S_{11} plot for parametric analysis. (a) S_{11} plot by varying distance between antenna and PRS with parasitic patches 'dx'. (b) S_{11} plot by varying parasitic patch size Rx.

3. SIMULATED AND MEASURED RESULTS

The results were simulated using CST Studio Suite 2021. The reflection coefficient (S_{11}) measurement was done at the facility provided by IIT, Bombay using Agilent 8722ET vector network analyser (VNA). The radiation pattern measurement was done at the facility provided by BITS Pilani, Goa using anechoic chamber measurement setup. A bidirectional, CPW-fed dumbbell-shaped slot antenna with PRS with parasitic patches was fabricated and tested. The simulated and measured S_{11} plots for the three configurations of antenna are shown in Figs. 5(a), (b), and (c). Fig. 5(d) shows the simulated and measured gains for the three configurations of antenna. The basic dumbbell-shaped antenna shows the bandwidth of 4.12 GHz (4.21–8.33 GHz) with percentage bandwidth of 65.70%, and the measured gain is 3.01 dBi at 7.6 GHz. For the antenna with PRS with parasitic patches on top, the measured bandwidth is 4.01 GHz (8.44–4.43 GHz) with percentage bandwidth of 62.31%, and the measured gain is 5.16 dBi at 7.6 GHz. For antenna with PRS with parasitic patches on top and bottom, the measured bandwidth is 4.11 GHz (8.59–4.48 GHz) with percentage bandwidth of 62.89%, and the measured gain is 5.61 dBi at 8 GHz. The maximum measured gain is around 6 dBi for the antenna with PRS patches.

Figures 6, 7, and 8(a), (b), and (c) show the normalized radiation patterns simulated and measured for frequencies 5.14 GHz, 6.175 GHz, and 7.5 GHz. The measured cross-polarization level is −36.31 dB, −29.27 dB, and −17.16 dB, respectively. By adding PRS with parasitic patches on top of the antenna, the cross-polarization improves at higher frequencies reducing it to −22.13 dB (7.5 GHz) as shown in Fig. 6. With the addition of PRS with parasitic patches, the cross-polarization further improves to −26.27 dB (7.5 GHz) as seen in Fig. 8, and the radiation pattern also improves making it radiate evenly. The antenna radiates evenly in two directions making it bidirectional with a difference of < 1 dB in

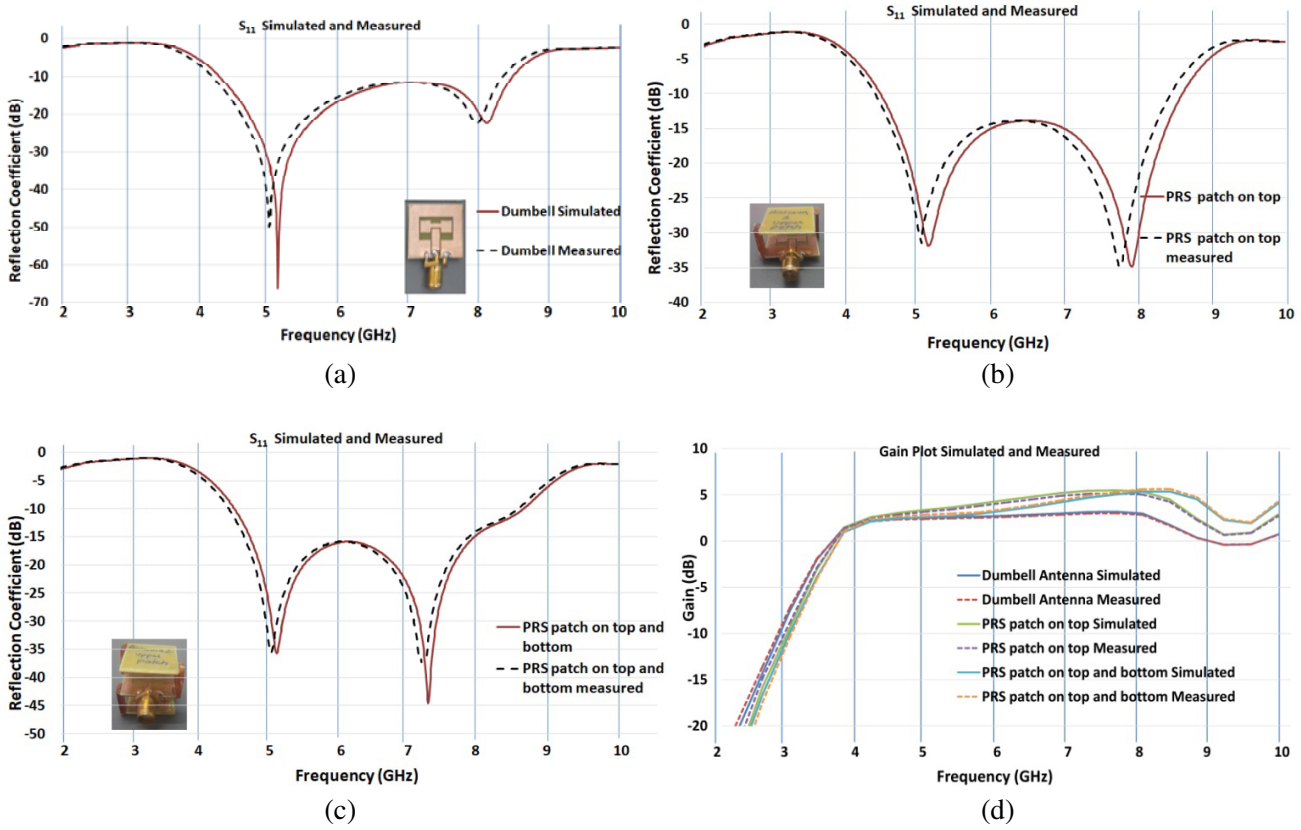

Figure 5. Measured and simulated results. (a) S_{11} plot for basic dumbbell shaped antenna. (b) S_{11} plot for antenna with PRS with parasitic patches on top. (c) S_{11} plot for antenna with PRS with parasitic patches on top and bottom. (d) Gain plot for all three configurations of antenna.

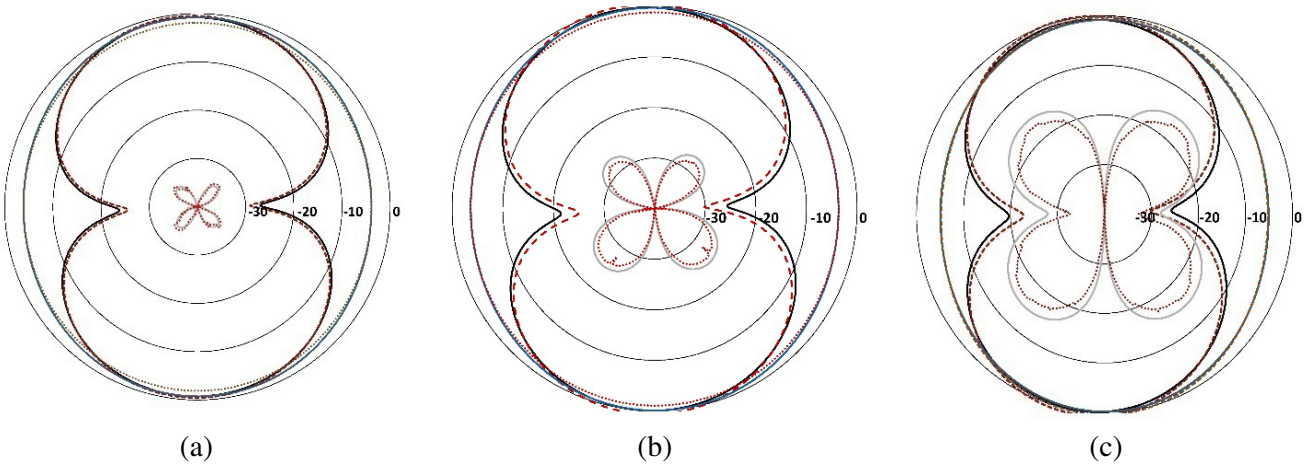

Figure 6. Measured and simulated radiation pattern of basic dumbbell shaped antenna. (a) 5.14 GHz. (b) 6.175 GHz. (c) 7.5 GHz.

the main lobe. The radiation patterns of the antenna are stable and symmetrical in both planes. The measured results are in close agreement with simulated ones.

The comparative analysis in Table 1 indicates that the proposed work has electrically small dimensions, and the bandwidth, gain, and radiation pattern are improved as compared to existing literature. The correlation between gain and bandwidth has been improved in the proposed work.

Table 1. Comparison of proposed antenna structure.

Ref.	Antenna size, Material used, Epsilon value	Frequency	BW	%BW	Gain
[21]	$0.8\lambda_o \times 0.46\lambda_o \times 0.02\lambda_o$ (CPW Fed Slot Antenna) FR-4 4.4	4.21–5.97 GHz	1.76 GHz	34.50%	4.5 dBi at 5.6 GHz between 4–4.58 dBi
[22]	$0.21\lambda_o \times 0.16\lambda_o \times 0.013\lambda_o$ (CPW Fed Slot Antenna) FR-4 4.4	2.07–2.77 GHz 3.3–3.8 GHz 5.15–5.35 GHz 5.7–5.89 GHz	NM	NM	2.4–2.8 dBi 1.9–2.1 dBi 2.9–3.5 dBi 2.6–3.2 dBi
[23]	$1.08\lambda_o \times 1.08\lambda_o \times 0.076\lambda_o$ (Single Layer on Same Substrate) Rogers 4350B 3.66	4.81–9.69 GHz	4.88 GHz	67.31%	9.18 dBi
[24]	$0.95\lambda_o \times 0.95\lambda_o \times 0.05\lambda_o$ (Single Layer Single Side Multiple Substrate) Rogers RO4003C 3.55	9.13–11.4 GHz	2.27 GHz	22.11%	8.4 dBi
[25]	$1.07\lambda_o \times 1.07\lambda_o \times 0.06\lambda_o$ (Single Layer Single Side Multiple Substrate) FR-4 4.4	3.26–5.84 GHz	2.58 GHz	56.7%	11.1 dBi
[26]	$0.47\lambda_o \times 0.47\lambda_o \times 0.025\lambda_o$ (Single Layer Single Side Multiple Substrate) FR-4 4.4	3.6–6.1 GHz	2.5 GHz	51.54%	7.87 dBi
[27]	$0.675\lambda_o \times 0.72\lambda_o \times 0.036\lambda_o$ (Single Layer Double Side Multiple Substrate) FR-4 4.4	6.5–8.3 GHz	2.05 GHz	24.32%	6.25 dBi
[28]	$1.03\lambda_o \times 0.78\lambda_o \times 0.021\lambda_o$ (Single Layer Double Side with lumped elements Multiple Substrate) FR-4 4.4	8.15–13.2 GHz	5.05 GHz	47.31%	7.8 dBi
[29]	$0.75\lambda_o \times 1.05\lambda_o$ Thickness $0.13\lambda_o$ (Double Layer Single Side on Multiple Substrate) Rogers 5880 2.2	5.85–10.52 GHz	4.67 GHz	57.1%	8.8 dBi
[30]	$1.28\lambda_o \times 1.28\lambda_o \times 0.68\lambda_o$ (Double Layer Single Side Multiple Substrate) FR4 4.4	8.2–12.5 GHz	4.1 GHz	44.00%	13 dBi
[31]	$0.81\lambda_o \times 0.81\lambda_o \times 0.114\lambda_o$ (Double Layer Double Side Multiple Substrate) FR4 4.2	2.1–2.7 GHz	0.6 GHz	25.00%	5 dBi
PW	$0.34\lambda_o \times 0.34\lambda_o \times 0.027\lambda_o$ (Basic Dumbell Antenna) $0.34\lambda_o \times 0.34\lambda_o \times 0.32\lambda_o$ (Antenna with PRS on top and bottom) FR4 4.4	Basic Dumbbell Antenna — 4.21–8.33 GHz Antenna with PRS on top — 4.43–8.44 GHz Antenna with PRS on top and bottom — 4.48–8.59 GHz	4.12 GHz 4.01 GHz 4.11 GHz	65.70% 62.31% 62.89%	3.01 dBi 5.16 dBi 5.61 dBi

NM — Not Mentioned, PW — Proposed Work

As compared to literature from [21, 23–31] size of the basic antenna is considerably reduced. The designed antenna structure with parasitic patches on top and bottom improves the percentage bandwidth as compared to [21, 24–31]. There is considerable improvement in the gain and radiation pattern characteristics as compared to [21, 22, 31]. The proposed work with PRS on top and bottom of the feed antenna also has a flat gain response for the complete band and the gain improvement around 3 dBi as compared to the basic feed antenna. Overall, the proposed CPW-fed slot antenna with parasitic patches on top and bottom provides better radiation characteristics than existing literature.

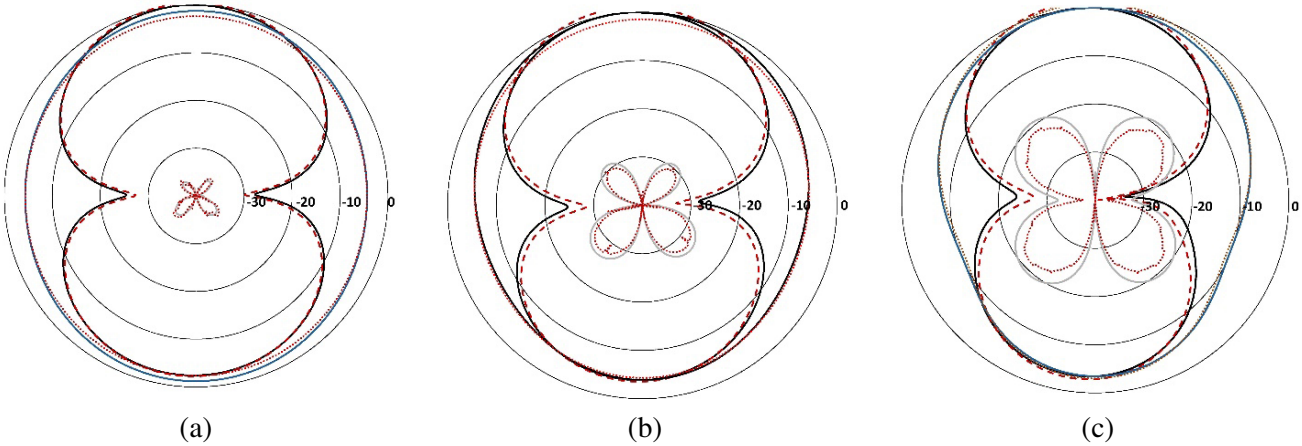

Figure 7. Measured and simulated radiation pattern of antenna with PRS with parasitic patch on top. (a) 5.14 GHz. (b) 6.175 GHz. (c) 7.5 GHz.

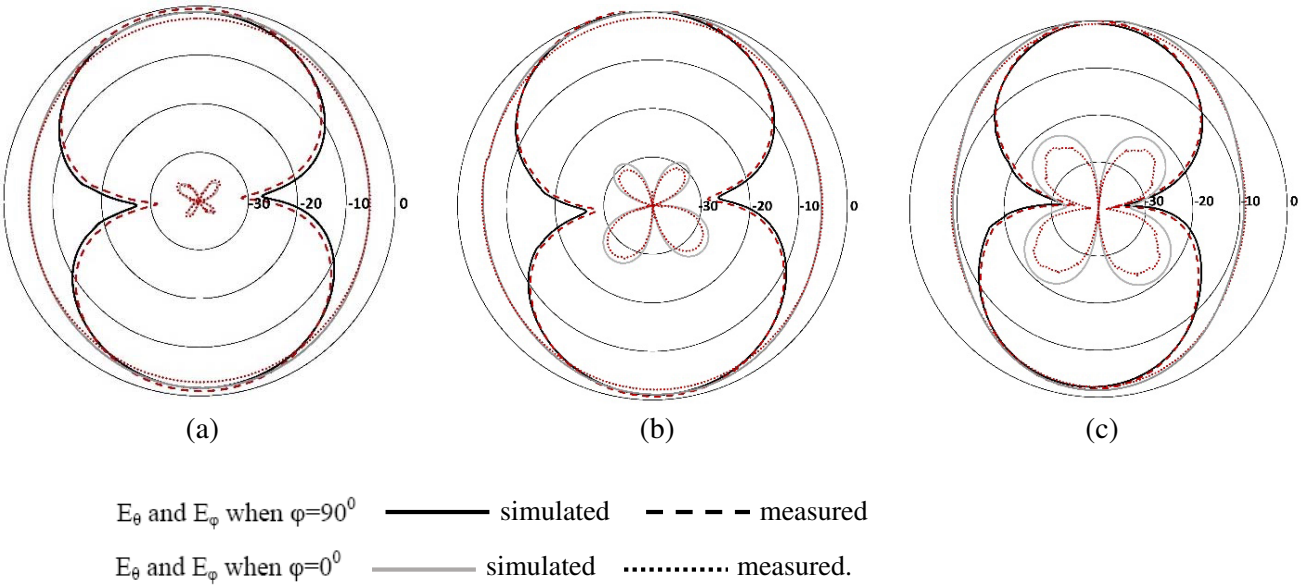

Figure 8. Measured and simulated radiation pattern of antenna with PRS with parasitic patch on top and bottom. (a) 5.14 GHz. (b) 6.175 GHz. (c) 7.5 GHz.

4. CONCLUSION

A bidirectional, CPW-fed dumbbell-shaped slot antenna with PRS with parasitic patches for gain, bandwidth, and radiation pattern improvement has been proposed and demonstrated successfully. Wideband performances have been achieved with bandwidths of 4.12 GHz, 4.01 GHz, and 4.11 GHz with percentage bandwidths of 65.70%, 62.31%, and 62.89% for the three configurations. The radiation pattern clearly indicates the bidirectional nature of the designed antenna. The variation in the main lobe is less than 1 dB in the two directions. The gain improvement is considerable with maximum gain achieved around 6 dBi. The gain variation over the complete band is less than 3 dB which makes the antenna a flat gain antenna. The radiation pattern improves by adding PRS with parasitic patches on top and bottom. The presented structure has a wide applications in C band which houses many standards and applications. The measured results substantiate validity of the design and concept. Furthermore, the antenna structure designed in this paper is less complex and has a low profile.

REFERENCES

1. ETSI, "Broadband radio access networks (BRAN); HIPERLAN type 2 technical specifications; physical layer (PHY)," Tech. Rep. DTS/BRAN-0023003, European Telecommunications Standards Institute, Sophia Antipolis, France, Oct. 1999.
2. O'Hara, B. and A. Petrick, *The IEEE 802.11 Handbook: A Designer's Companion*, IEEE Press, New York, NY, USA, 1999.
3. Diels, W., K. Vaesen, P. Wambacq, et al., "Single-package integration of RF blocks for a 5 GHz WLAN application," *IEEE Transactions on Advanced Packaging*, Vol. 24, No. 3, 384–391, 2001.
4. IEEE 802.11, "Wireless access method and physical layer specifications," New York, NY, USA, Sep. 1994.
5. Wong, K.-L., *Compact and Broadband Microstrip Antennas*, John Wiley & Sons, New York, NY, USA, 2002.
6. Huynh, T. and K.-F. Lee, "Single-layer single-patch wideband microstrip antenna," *Electronics Letters*, Vol. 31, No. 16, 1310–1312, 1995.
7. Wong, K.-L. and W.-H. Hsu, "Broadband triangular microstrip antenna with U-shaped slot," *Electronics Letters*, Vol. 33, No. 25, 2085–2087, 1997.
8. Guo, Y. X., K. M. Luk, and K. F. Lee, "L-probe proximity-fed short-circuited patch antennas," *Electronics Letters*, Vol. 35, No. 24, 2069–2070, 1999.
9. Tong, K. F., K. M. Luk, K. F. Lee, and R. Q. Lee, "A broad-band U-slot rectangular patch antenna on a microwave substrate," *IEEE Transactions on Antennas and Propagation*, Vol. 48, No. 6, 954–960, 2000.
10. Guo, Y.-X., K.-M. Luk, K.-F. Lee, and R. Chair, "A quarter-wave U-shaped patch antenna with two unequal arms for wideband and dual-frequency operation," *IEEE Transactions on Antennas and Propagation*, Vol. 50, No. 8, 1082–1087, 2002.
11. Yen, M.-H., P. Hsu, and J.-F. Kiang, "Analysis of a CPW-fed slot ring antenna," *Proc. APMC 2001 Int. Conf.*, 1267–1270, 2001.
12. Tehrani, H. and K. Chang, "Multifrequency operation of microstrip-fed slot-ring antennas on thin low-dielectric permittivity substrates," *IEEE Trans. Antennas Propag.*, Vol. 50, No. 9, 1299–1308, Sep. 2002.
13. Chen, J.-S., "Studies of CPW-fed equilateral triangular-ring slot antennas and triangular-ring slot coupled patch antennas," *IEEE Trans. Antennas Propag.*, Vol. 53, No. 7, 2208–2211, Jul. 2005.
14. Trentini, G. V., "Partially reflecting sheet arrays," *IRE Trans. Antennas Propag.*, Vol. 4, No. 4, 666–671, Oct. 1956.
15. Feresidis, A. P. and J. C. Vardaxoglou, "High gain planar antenna using optimised partially reflective surfaces," *Proc. Inst. Elect. Eng. Microw. Antennas Propag.*, Vol. 148, No. 6, 345–350, Dec. 2001.
16. Foroozesh, N. A. and L. Shafai, "Investigation into the effects of the patch-type fss superstrate on the high-gain cavity resonance antenna design," *IEEE Trans. Antennas Propag.*, Vol. 58, No. 2, 258–270, Feb. 2010.
17. Alexopoulos, N. and D. Jackson, "Fundamental superstrate (cover) effect on printed circuit antennas," *IEEE Trans. Antennas Propag.*, Vol. 32, No. 8, 807–816, Aug. 1984.
18. Lee, R. Q. and K. F. Lee, "Experimental study of the two-layer electromagnetically coupled rectangular patch antenna," *IEEE Trans. Antennas Propag.*, Vol. 38, No. 8, 1298–1302, Aug. 1990.
19. Egashira, S. and E. Nishiyama, "Stacked microstrip antenna with wide bandwidth and high gain," *IEEE Trans. Antennas Propag.*, Vol. 44, No. 11, 1533–1534, Nov. 1996.
20. Foroozesh, A. and L. Shafai, "2-D truncated periodic leaky-wave antennas with reactive impedance surface ground," *Proc. IEEE AP-S Int. Symp.*, 15–18, Albuquerque, NM, Jul. 9–14, 2006.
21. Yu, C.-C. and X.-C. Lin, "A wideband single chip inductor-loaded CPW-fed inductive slot antenna," *IEEE Trans. Antennas Propag.*, Vol. 56, No. 5, 1498–1501, May 2008.

22. Sun, X., G. Zeng, H.-C. Yang, and Y. Li, "A compact quadband CPW-fed slot antenna for M-WiMAX/WLAN applications," *IEEE Antennas and Wireless Propagation Letters*, Vol. 11, 395–398, Apr. 2012.
23. Wang, J., H. Wong, Z. Ji, and Y. Wu, "Broadband CPW-fed aperture coupled metasurface antenna," *IEEE Antennas and Wireless Propagation Letters*, Vol. 18, No. 3, 517–520, Mar. 2019.
24. Liao, H.-P. and S.-Y. Chen, "Bandwidth and gain enhancement of CPW-fed slot antenna using a partially reflective surface formed by two-step tapered dipole unit cells," *2019 IEEE Asia-Pacific Microwave Conference (APMC)*, 2019.
25. Zhou, E., Y. Cheng, F. Chen, H. Luo, and X. Li, "Low-profile high-gain wideband multi-resonance microstrip-fed slot antenna with anisotropic metasurface," *Progress In Electromagnetics Research*, Vol. 175, 91–104, 2022.
26. Kumar, A., A. De, and R. K. Jain, "Gain enhancement using modified circular loop FSS loaded with slot antenna for sub-6 GHz 5G application," *Progress In Electromagnetics Research Letters*, Vol. 98, 41–48, 2021.
27. Paik, H., S. K. Mishra, C. M. Sai Kumar, and K. Premchand, "High performance CPW fed printed antenna with double layered frequency selective surface reector for bandwidth and gain improvement," *Progress In Electromagnetics Research Letters*, Vol. 102, 47–55, 2022.
28. Bhattacharya, A., B. Dasgupta, and R. Jyoti, "Design and analysis of ultrathin X-band frequency selective surface structure for gain enhancement of hybrid antenna," *International Journal of RF and Microwave Computer-Aided Engineering*, e22505, Nov. 2020.
29. Cheng, Y.-F., X. Ding, X. Xu, X. Zhong, and C. Liao, "Design and analysis of a bow-tie slot-coupled wideband metasurface antenna," *IEEE Antennas and Wireless Propagation Letters*, Vol. 18, No. 7, 1342–1346, Jul. 2019.
30. Kanjanasit, K. and C. Wang, "A wideband resonant cavity antenna assembled using a micromachined CPW-fed patch source and a two-layer metamaterial superstrate," *IEEE Trans. on Components, Packaging and Manufacturing Tech.*, Vol. 9, No. 6, 1142–1150, Jun. 2019.
31. Chaimool, S., C. Rakluea, and P. Akkaraekthalin, "Mu-near-zero metasurface for microstrip-fed slot antennas," *Appl. Phys.*, Vol. 112, 669–675, Apr. 2013.